Xeroderma pigmentosum group C protein interacts with histones: regulation by acetylated states of histone H3

Kakumu, Erina ; Nakanishi, Seiya ; Shiratori, Hiromi M. ; Kato, Akari ; Kobayashi, Wataru ; Machida, Shinichi ; Yasuda, Takeshi ; Adachi, Naok…

(Citation)
Genes to Cells,22(3):310-327

(Issue Date)
2017-03

(Resource Type)
journal article

(Version)
Version of Record

Genes to Cells

Xeroderma pigmentosum group C protein interacts with histones: regulation by acetylated states of histone H3

Erina Kakumu[1,2], Seiya Nakanishi[1,2], Hiromi M. Shiratori[1,3], Akari Kato[1,2], Wataru Kobayashi[4], Shinichi Machida[4], Takeshi Yasuda[5], Naoko Adachi[6], Naoaki Saito[6], Tsuyoshi Ikura[7], Hitoshi Kurumizaka[4], Hiroshi Kimura[8], Masayuki Yokoi[1,2,3], Wataru Sakai[1,2,3] and Kaoru Sugasawa[1,2,3]*

[1]*Division of Genomic Functions and Dynamics, Biosignal Research Center, Kobe University, 1-1 Rokkodai-cho, Nada-ku, Kobe, Hyogo 657-8501, Japan*
[2]*Department of Biology, Graduate School of Science, Kobe University, 1-1 Rokkodai-cho, Nada-ku, Kobe, Hyogo 657-8501, Japan*
[3]*Department of Biology, Faculty of Science, Kobe University, 1-1 Rokkodai-cho, Nada-ku, Kobe, Hyogo 657-8501, Japan*
[4]*Graduate School of Advanced Science and Engineering, Waseda University, 2-2 Wakamatsu-cho, Shinjuku-ku, Tokyo 162-8480, Japan*
[5]*National Institute for Quantum and Radiological Science and Technology, 4-9-1 Anagawa, Inage-ku, Chiba 263-8555, Japan*
[6]*Division of Molecular Pharmacology, Biosignal Research Center, Kobe University, 1-1 Rokkodai-cho, Nada-ku, Kobe, Hyogo 657-8501, Japan*
[7]*Department of Mutagenesis, Radiation Biology Center, Kyoto University, Yoshidakonoe-cho, Sakyo-ku, Kyoto 606-8501, Japan*
[8]*Graduate School of Bioscience and Biotechnology, Tokyo Institute of Technology, 4259 Nagatsuta-cho, Midori-ku, Yokohama 226-8501, Japan*

In the mammalian global genome nucleotide excision repair pathway, two damage recognition factors, XPC and UV-DDB, play pivotal roles in the initiation of the repair reaction. However, the molecular mechanisms underlying regulation of the lesion recognition process in the context of chromatin structures remain to be understood. Here, we show evidence that damage recognition factors tend to associate with chromatin regions devoid of certain types of acetylated histones. Treatment of cells with histone deacetylase inhibitors retarded recruitment of XPC to sites of UV-induced DNA damage and the subsequent repair process. Biochemical studies showed novel multifaceted interactions of XPC with histone H3, which were profoundly impaired by deletion of the N-terminal tail of histone H3. In addition, histone H1 also interacted with XPC. Importantly, acetylation of histone H3 markedly attenuated the interaction with XPC *in vitro*, and local UV irradiation of cells decreased the level of H3K27ac in the damaged areas. Our results suggest that histone deacetylation plays a significant role in the process of DNA damage recognition for nucleotide excision repair and that the localization and functions of XPC can be regulated by acetylated states of histones.

Introduction

Genomic DNA is continuously damaged by various factors originating from both endogenous and environmental sources. In general, DNA damage has detrimental impacts on fundamental genomic functions and dynamics, including transcription, replication and chromosomal segregation. As the primary defense against DNA damage, cells have evolved multiple DNA repair pathways that play pivotal roles in prevention of genomic instability (e.g., mutations and chromosomal aberrations), cellular senescence and apoptosis.

Nucleotide excision repair (NER) is the most versatile DNA repair pathway, which covers a broad range of helix-distorting DNA lesions that do not

Communicated by: Fumio Hanaoka
**Correspondence:* ksugasawa@garnet.kobe-u.ac.jp
Conflicts of interest: The authors declare that no competing interests exist.

DOI: 10.1111/gtc.12479

share any common chemical structures (Gillet & Schärer 2006). Substrates of NER include ultraviolet light (UV)-induced DNA photolesions, such as cyclobutane pyrimidine dimers (CPDs) and pyrimidine (6-4) pyrimidone photoproducts (6-4PPs), intrastrand cross-links caused by bifunctional alkylating agents, and bulky base adducts that can be induced by numerous chemical carcinogens. Importantly, hereditary defects in NER have been implicated in several human autosomal recessive disorders, such as xeroderma pigmentosum (XP) (de Boer & Hoeijmakers 2000). Patients with XP are clinically characterized by photosensitivity of skin and a very high susceptibility to UV-induced skin cancer. Seven NER-deficient genetic complementation groups (XP-A through G) have been identified for XP, and all of the responsible gene products are directly involved in the NER machinery (Friedberg 2001; Schärer 2013).

To properly initiate DNA repair reactions, it is crucial to detect and locate precisely a small number of relevant lesions buried in normal DNA, which is present in large excess. Mammalian NER uses several alternative mechanisms for DNA damage recognition. At transcriptionally active loci, the repair reaction is efficiently triggered by blockage of elongating RNA polymerase at a lesion on the transcribed strand (Hanawalt & Spivak 2008; Lagerwerf *et al.* 2011). This transcription-coupled NER subpathway is thought to contribute to rapid recovery of cellular transcriptional activity after DNA damage, which prevents apoptosis. However, the majority of lesions throughout the genome are recognized by specialized DNA-binding factors in a transcription-independent fashion (Yang 2008). The latter subpathway, called global genome NER (GG-NER), prevents replication forks from colliding with lesions, thereby reducing the risk of genomic instability and carcinogenesis.

In mammals, two XP-related protein factors play key roles in lesion recognition for GG-NER. The XPC protein complex (XPC–RAD23–CETN2 heterotrimer) is able to recognize and bind to DNA sites containing a wide variety of lesions, and its specific binding depends on the presence of disrupted or destabilized base pairs in the DNA duplex (Hey *et al.* 2002; Sugasawa *et al.* 2002; Brown *et al.* 2010; Yeo *et al.* 2012). When XPC forms a stable complex with DNA, it interacts only with intact bases that are prevented from normal base pairing, but not with the lesion itself (Sugasawa *et al.* 2001; Min & Pavletich 2007). This indirect mode of damage recognition underlies the extremely broad substrate specificity of GG-NER. However, the DDB1–DDB2 (XPE) heterodimer, also designated as UV-damaged DNA-binding protein (UV-DDB), is more specialized for recognition of UV-induced photolesions (Reardon *et al.* 1993; Payne & Chu 1994; Fujiwara *et al.* 1999; Wittschieben *et al.* 2005). In contrast to XPC, UV-DDB directly interacts with the affected bases themselves (Scrima *et al.* 2008), thereby promoting recruitment of XPC to sites with specific types of DNA damage (Fitch *et al.* 2003; Wang *et al.* 2004; Moser *et al.* 2005). UV-DDB is part of a Cullin4–RING ubiquitin ligase complex ($CRL4^{DDB2}$) (Shiyanov *et al.* 1999; Groisman *et al.* 2003; Kulaksiz *et al.* 2005; Fischer *et al.* 2011), and posttranslational protein modifications including ubiquitination (Sugasawa *et al.* 2005; Kapetanaki *et al.* 2006; Wang *et al.* 2006; Puumalainen *et al.* 2014; Matsumoto *et al.* 2015) and SUMOylation (Poulsen *et al.* 2013; Akita *et al.* 2015; van Cuijk *et al.* 2015) are involved in regulation of the UV-DDB-mediated damage recognition process. Regardless of the intervention by UV-DDB, XPC bound to a damaged site recruits the general transcription factor IIH (TFIIH) complex (Li *et al.* 1998; Yokoi *et al.* 2000; Araújo *et al.* 2001; Okuda *et al.* 2015). In concert with XPA, TFIIH checks for the presence of abnormal chemical structures in DNA, a process in which ATPase/helicase activities of XPB and XPD subunits play crucial roles (Sugasawa *et al.* 2009; Mathieu *et al.* 2010; Li *et al.* 2015). This damage verification process is important to avoid unnecessary incisions at damage-free sites, thereby ensuring the accuracy of the entire repair system.

Although the damage recognition mechanism of GG-NER has been well characterized at a molecular level, the *in vivo* regulation of the process, especially in the context of chromatin structures, remains to be elucidated (see a recent review by Polo & Almouzni 2015). In regulation of gene expression, higher-order chromatin structures are interconverted by writing and erasing various epigenetic marks, such as histone modifications and DNA methylation. In general, chromatin regions containing acetylated histones are more accessible to DNA-binding proteins, and therefore more transcriptionally competent, whereas transcriptionally inactive chromatin regions are highly condensed and often marked with methylation of DNA and histones. However, it remains unknown whether GG-NER is regulated in exactly the same way as transcription. Biochemical studies using cell-free NER systems showed that if a lesion is present within the nucleosome core, the interaction with XPC and the subsequent repair reaction are inhibited

(Hara *et al.* 2000; Yasuda *et al.* 2005), suggesting that histones may need to be evicted from sites of damage before XPC binding (Adam *et al.* 2015). By contrast, UV-DDB can bind the damage-containing nucleosome core, presumably by recognizing a flexible DNA backbone exposed to the outer surface (Osakabe *et al.* 2015), suggesting that UV-DDB may induce remodeling of the damaged nucleosome such that the lesion becomes accessible to XPC. Indeed, UV-DDB interacts with chromatin remodeling factors (Jiang *et al.* 2010; Pines *et al.* 2012) and various protein modification enzymes, including the histone acetyltransferases CBP/p300 (Datta *et al.* 2001; Rapić-Otrin *et al.* 2002), GCN5 (Martinez *et al.* 2001) and KAT7/HBO1/MYST2 (Matsunuma *et al.* 2015), the histone deacetylases HDAC1/2 (Zhao *et al.* 2014; Zhu *et al.* 2015) and poly(ADP-ribose) polymerase 1 (PARP1) (Pines *et al.* 2012; Robu *et al.* 2013), as well as the ubiquitin ligase mentioned above. However, it remains to be determined how these factors are coordinated to ensure appropriate modulation in time and space of chromatin structures for GG-NER. Notably, UV-induced 6-4PPs are removed almost completely from the genome even in the absence of UV-DDB, albeit with a considerable delay (Hwang *et al.* 1999; Tang *et al.* 2000; Moser *et al.* 2005), but it remains unclear how cells can sense the presence of lesions and alter chromatin structures before XPC interacts with the lesions.

In this study, we investigated the epigenetic characteristics of chromatin structures at sites where damage recognition for GG-NER occurs, and the results show interactions between XPC and histones. Our findings provide novel insights into the *in vivo* regulation of the damage recognition process.

Results

NER damage recognition factors associate with chromatin devoid of some acetylated histones

To examine features of chromatin structures where NER damage recognition occurs, we carried out chromatin immunoprecipitation (ChIP) experiments targeting XPC or DDB2. First, we used an *XPC*-deficient human cell line stably expressing the FLAG-tagged XPC (FLAG-XPC) protein at nearly physiological levels. In this cell line, the defect in GG-NER of the parental cells is corrected, as judged from removal of UV-induced 6-4PPs (Yasuda *et al.* 2007). When ChIP was carried out with this cell line and anti-FLAG antibody, coprecipitation of the downstream NER factor XPA was transiently increased after UV irradiation (Nishi *et al.* 2013). This interaction diminished to the background level at 3 h postirradiation, by which time repair of 6-4PPs was almost completed, thus validating our ChIP system.

This ChIP system was used to analyze histone modifications associating with FLAG-XPC. At various time points after UV irradiation, ChIP samples were prepared and subjected to Western blot analyses with antibodies that specifically recognized various histone modifications. For precise comparisons, aliquots of input chromatin fractions were analyzed in parallel, and each blot was reprobed with an anti-histone H3 pan antibody. As shown in Fig. 1A, amounts of histone H3 coprecipitated with FLAG-XPC were not significantly affected by UV irradiation, suggesting that XPC associates with chromatin even without exogenous DNA damage. Intriguingly, some types of histone acetylation, such as H3K14ac and H3K27ac, were substantially underrepresented in the ChIP fractions, regardless of UV irradiation. By contrast, other modifications, like H3K9me3, were detected at comparable levels, as expected from the amounts of histone H3 in the ChIP fractions.

Similar experiments were carried out with the normal human fibroblast cell line WI38 VA13 stably expressing FLAG-DDB2 (Fig. 1B). In contrast to XPC, the amounts of coprecipitated histone H3 transiently increased after UV irradiation, suggesting that DDB2 binds to chromatin in response to UV-induced DNA damage. However, FLAG-DDB2 interacted weakly with H3K14ac or H3K27ac. These results indicate that NER damage recognition factors tend to associate with chromatin regions that lack certain types of acetylated histones.

Inhibition of HDAC activities compromises GG-NER

The results described above raised the possibility that deacetylation of histones is involved in the process of damage recognition for GG-NER. To investigate the possible role of deacetylation, we examined the effects of histone deacetylase (HDAC) inhibitors on GG-NER. WI38 VA13 cells were treated for 6 h with various concentrations of the HDAC inhibitors trichostatin A (TSA) and sodium butyrate (NaBu). For both inhibitors, acetylated histones accumulated in a dose-dependent manner, as expected (Fig. 2A). In the presence of an effective concentration of TSA or NaBu, repair of UV-induced 6-4PPs was delayed

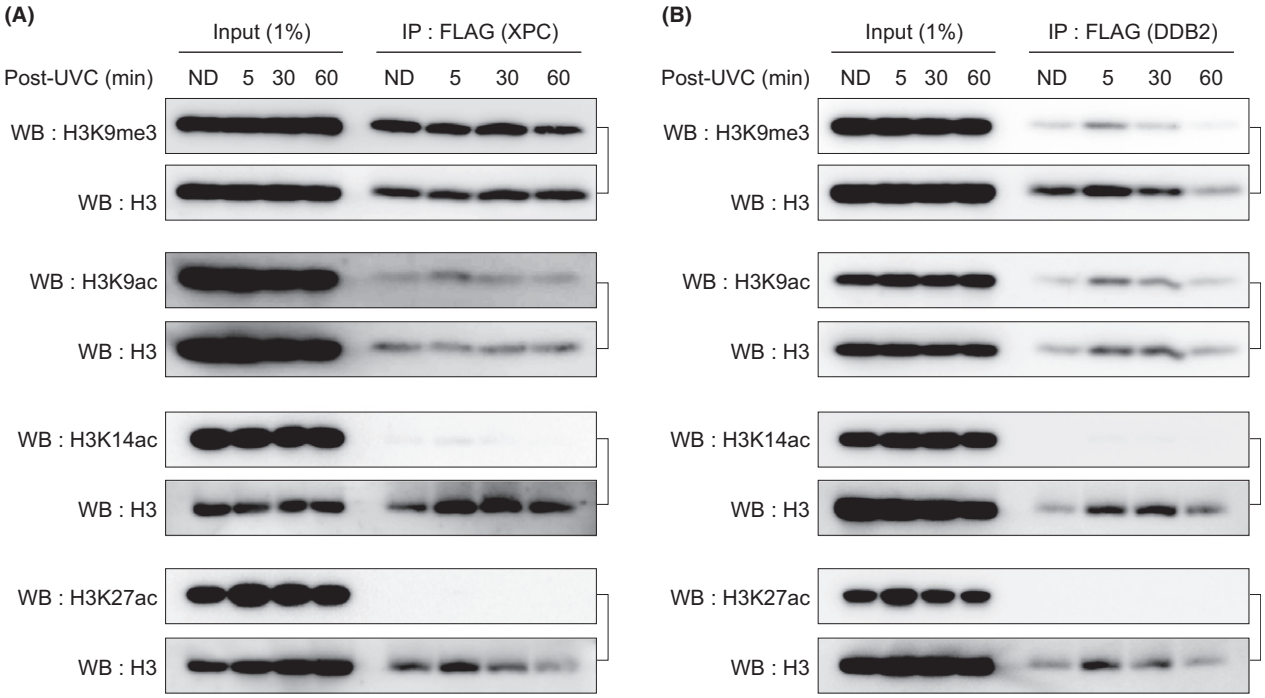

Figure 1 XPC and UV-DDB associate with chromatin lacking certain types of acetylated histones. Cells stably expressing FLAG-XPC (A) or FLAG-DDB2 (B) were treated with 10 J/m^2 UVC and incubated for the indicated time periods (ND: sham-irradiated samples), and then ChIP was carried out with anti-FLAG antibody beads. Bound fractions and aliquots of the input chromatin fractions were subjected to Western blot analyses with antibodies specific for various histone modifications. Each blot was reprobed with anti-H3 pan antibody.

(Fig. 2B), whereas the initial level of the generated lesions was unaffected (data not shown). Next, we investigated how HDAC inhibitors would affect recruitment of NER damage recognition factors to sites with UV-induced photolesions. For this purpose, we used a local UV irradiation system in which UVC light was focused by a reflective objective lens to a certain area within the nucleus under a fluorescence microscope. Local UV was applied to the cells stably expressing EGFP-tagged XPC (EGFP-XPC) or mKO1-tagged DDB2 (DDB2-mKO1). Time-lapse imaging and quantitative measurement of fluorescence intensities in the irradiated area showed that accumulation of EGFP-XPC, but not DDB2-mKO1, was significantly retarded by treatment with the HDAC inhibitors (Fig. 2C,D). These results indicate that HDAC activities have stimulatory effects on the damage recognition process involving XPC.

XPC directly interacts with histones

To further investigate functional interactions between XPC and chromatin, we searched for interacting partners of XPC. To this end, we carried out sequential affinity purification of HA- and FLAG-tagged XPC stably expressed in HeLa S3 cells. Initial analyses with mass spectrometry indicated that histones H3 and H4 existed in the XPC complexes. The presence of histone H3 in the purified complex was confirmed by Western blot analysis (Fig. 3A).

This finding prompted us to investigate whether XPC directly interacts with histones. For this purpose, we first carried out far-Western blot analyses. A total histone fraction was prepared from cultured cells using the H_2SO_4 extraction method (Fig. 3B). This histone fraction was separated on a SDS polyacrylamide gel, transferred to a membrane filter and incubated with purified recombinant XPC–RAD23B complex. Two major bands were detected with an anti-XPC antibody: the faster migrating one was identified as histone H3 because recombinant human H3.1 gave rise to a signal with the same mobility (Fig. 3B). Intriguingly, truncation of the N-terminal 27 amino acids from histone H3.1 dramatically reduced this interaction. For the slower migrating

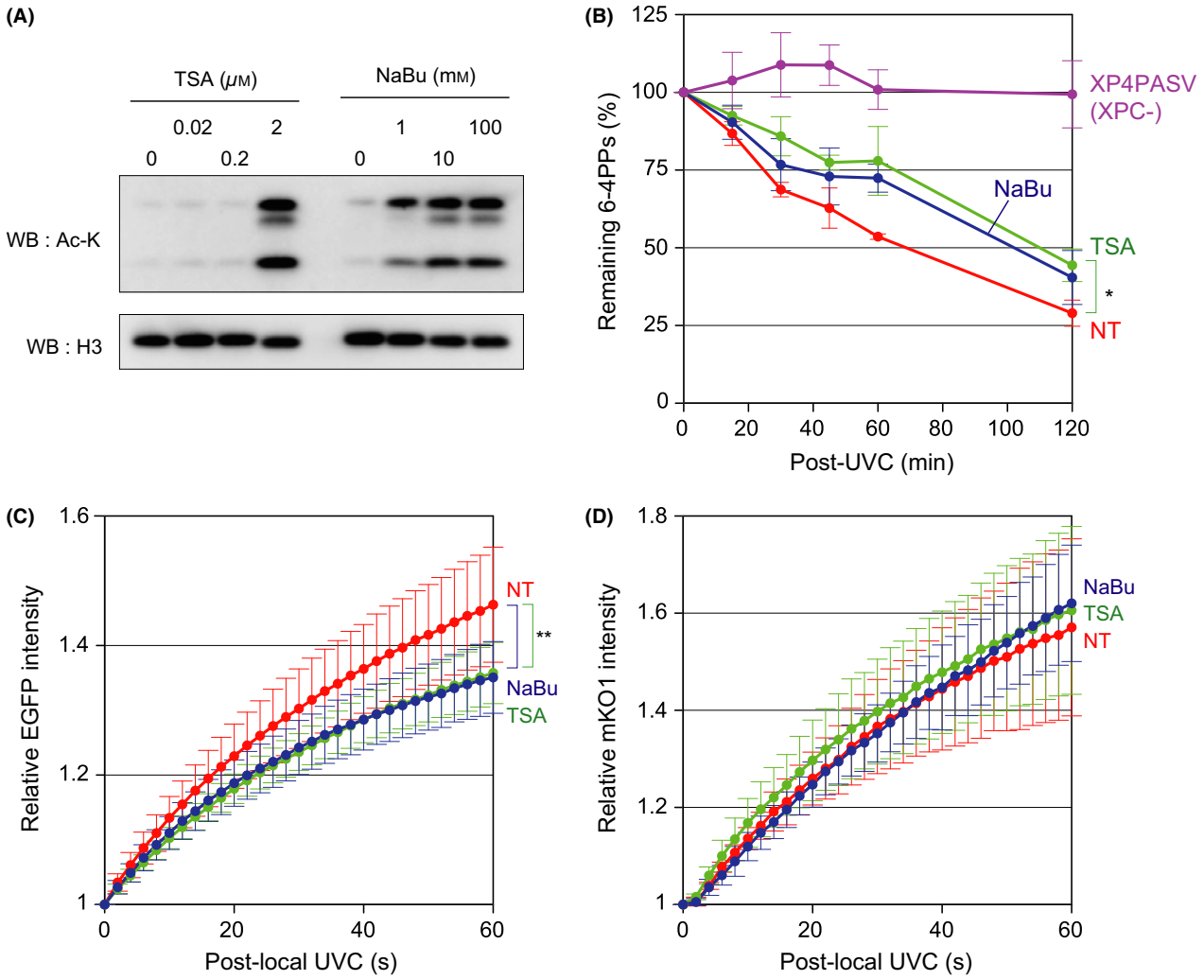

Figure 2 Inhibition of histone deacetylases (HDAC) compromises GG-NER. (A) WI38 VA13 cells were treated for 6 h with the indicated concentrations of HDAC inhibitors. Crude chromatin fractions were prepared and subjected to Western blot analyses with anti-acetyl-lysine (Ac-K) and anti-histone H3 antibodies. (B) WI38 VA13 cells were treated for 6 h with 2 μM TSA or 10 mM NaBu, irradiated with 10 J/m^2 UVC and further incubated for the indicated times in the presence of the same HDAC inhibitors. As controls, WI38 VA13 cells not treated with HDAC inhibitors (NT) and *XPC*-deficient XP4PASV cells were analyzed in parallel. Genomic DNA was purified from each sample, and the amount of remaining 6-4PPs was quantified with lesion-specific antibody. Mean values and standard errors were calculated from three independent experiments. Student's *t*-tests showed that the observed difference between the NT and TSA samples was statistically significant. *$P < 0.05$. (C) Local UVC irradiation was carried out under a fluorescence microscope in XP4PASV cells stably expressing EGFP-XPC, which were treated for 6 h with or without HDAC inhibitors (2 μM TSA or 10 mM NaBu). Time-lapse images were acquired, and the ratio of fluorescence intensities in the irradiated vs. unirradiated areas was calculated for each time point. Mean values and standard errors were calculated from measurements from 30 cells. Student's *t*-tests were carried out to assess statistical significance of the observed differences. **$P < 5 \times 10^{-7}$. (D) WI38 VA13 cells stably expressing DDB2-mKO1 were used for experiments similar to those in (C).

band, the mobility suggested histone H1; this assignment was confirmed by fractionation of histones into core and linker histones, and also by comparison with recombinant histone H1.2 (Fig. 3C).

Next, we sought to determine which part of XPC–RAD23B was responsible for the observed interactions with histones. We did not observe significant interaction with RAD23B alone (data not

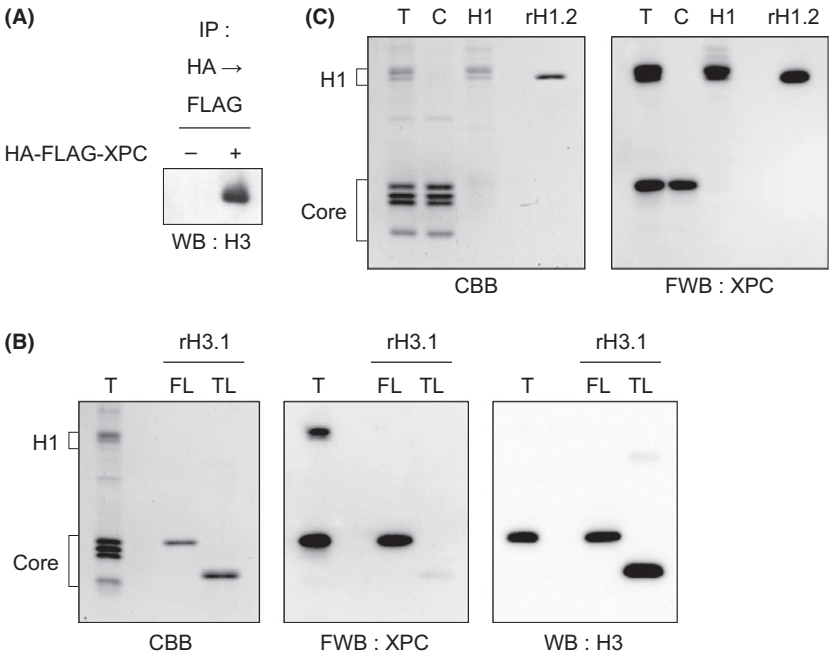

Figure 3 Direct physical interactions between XPC and histones. (A) Sequential immunoprecipitation was carried out with anti-HA and anti-FLAG antibody beads from nuclear extracts of HeLa S3 cells with (+) or without (–) ectopic expression of XPC fused to the HA-FLAG tandem tag. The resultant protein complexes were subjected to Western blot analysis with anti-histone H3 antibody. (B) Total histone fraction prepared from human cultured cells (T) and recombinant histone H3.1 proteins, full-length (FL) and N-terminal tail-less (TL), were subjected to far-Western blot analysis with purified XPC–RAD23B complex. (C) In addition to total histones, core (C) and linker (H1) histone fractions were prepared from cells and subjected to far-Western blot analysis with XPC–RAD23B along with recombinant histone H1.2.

shown), suggesting that XPC serves as the main platform for this binding. The XPC protein comprises four evolutionarily conserved domains, which are crucially involved in DNA damage recognition: the transglutaminase homology domain (TGD) and three consecutive β-hairpin domains (BHD1, BHD2 and BHD3) (Min & Pavletich 2007). In human XPC, TGD is divided into two parts; the intervening region is poorly conserved in terms of length and amino acid sequence and is predicted to be structurally disordered (Fig. 4A). Based on this information, we prepared several truncated versions of the XPC protein: one N-terminal (amino acids 1–324) and two C-terminal (513–870 and 513–940) fragments. These mutant XPC proteins were subjected to far-Western blot analyses, in which recombinant histone H3.1 or H1.2 was incubated with the mutant XPC proteins transferred onto membrane filters. Only the N-terminal fragment of XPC interacted with histones H3.1 and H1.2 under these conditions (Fig. 4B,C). We further truncated the N-terminal end of the XPC fragment, which is predicted to be disordered (Fig. 4A). The interactions with both histones were markedly attenuated by deletion of 64 amino acids and reduced to undetectable levels by deletion of 127 amino acids (Fig. 4D,E). Taken together, under our far-Western blotting conditions, the very N-terminal part of XPC was involved in the interactions with histones H3 and H1.

Multiple sites in XPC interact with histone H3

Although our far-Western blot analyses showed some interactions, we could not exclude the possibility that additional interactions might occur if XPC was not denatured. Therefore, we carried out pull-down assays to examine the XPC–histone interactions. When recombinant histone H3.1 was immobilized on magnetic beads, specific binding of the XPC–RAD23B complex was observed as expected (Fig. 5A). However, histone H1.2 failed to specifically pull down a detectable amount of XPC–-RAD23B with this system, at least under the conditions we tested (data not shown).

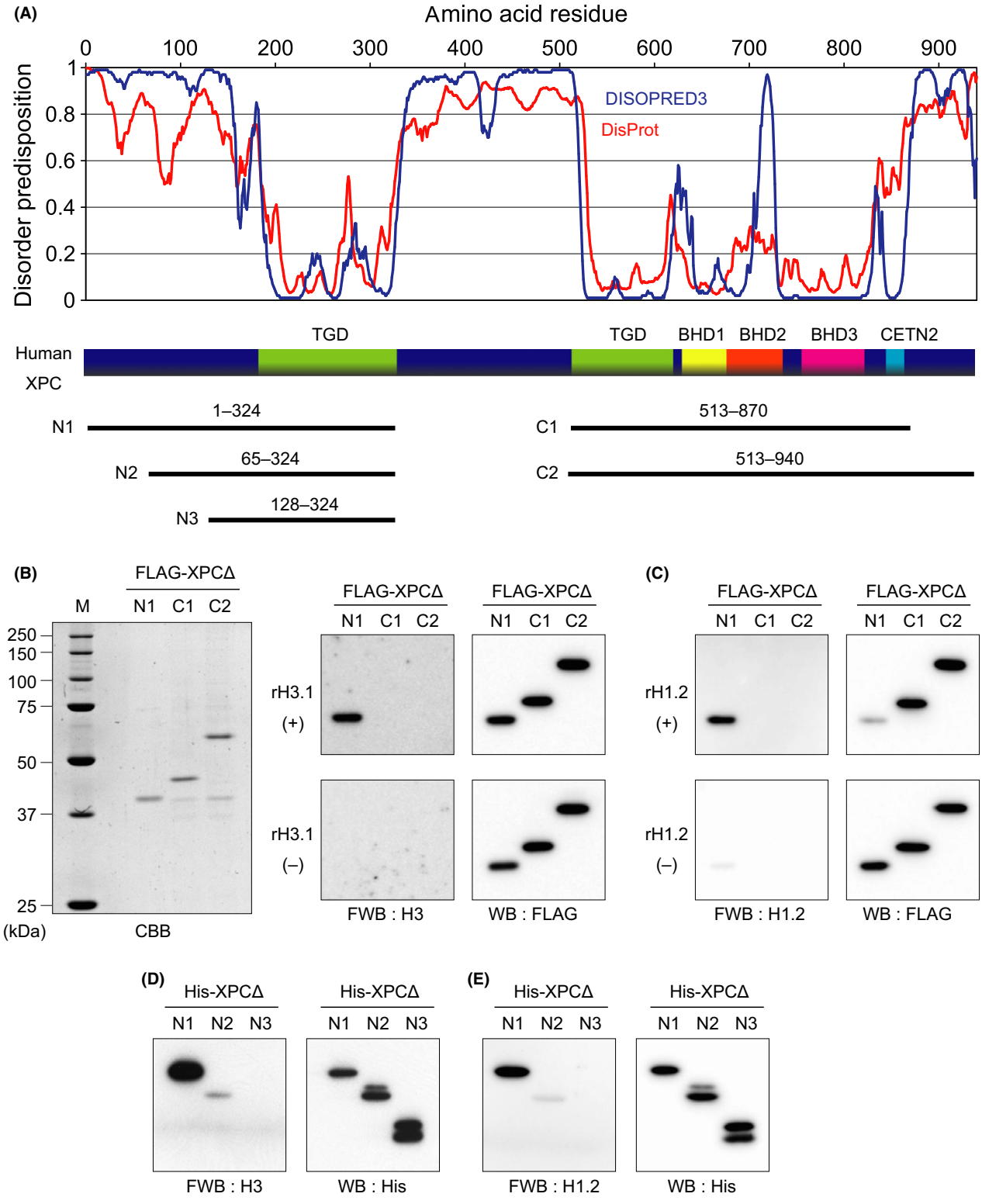

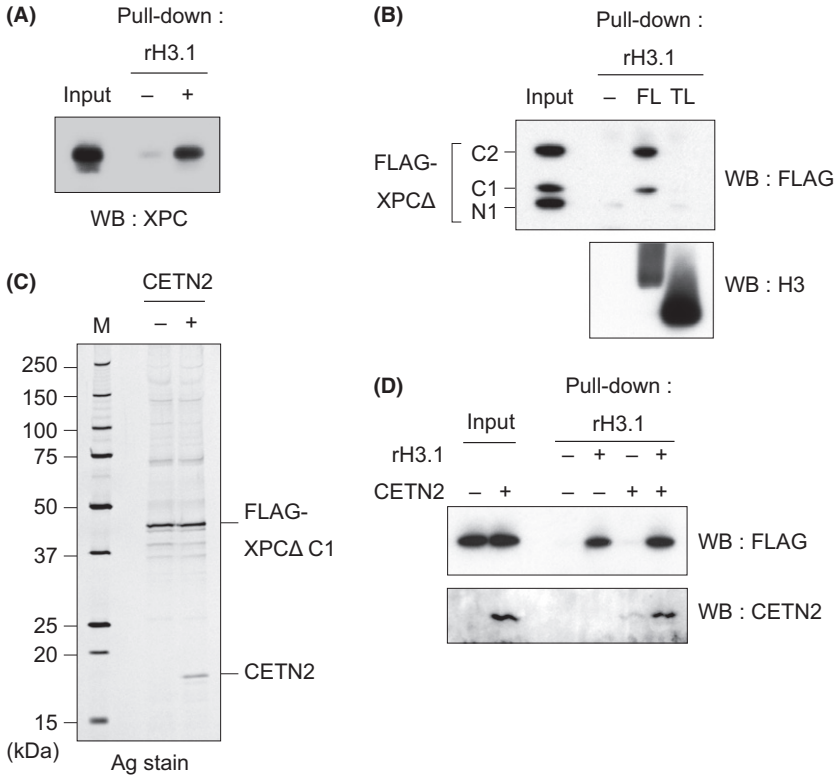

Figure 5 The C-terminal part of XPC interacts with histone H3 in pull-down assays. (A) Paramagnetic beads immobilized with (+) or without (−) recombinant histone H3.1 were used to pull down the XPC–RAD23B complex. XPC protein in the input and bound fractions was detected by Western blotting. (B) A mixture of three FLAG-tagged XPC deletion mutants (N1, C1 and C2) was subjected to pull-down assays without (−) or with histone H3.1, full-length (FL) or tail-less (TL). As a control, histone H3 in the bound fractions was also detected. (C) The FLAG-tagged XPC deletion mutant C1 was purified with (+) or without (−) CETN2 and then subjected to SDS-PAGE followed by silver staining. (D) Protein fractions shown in (C) were subjected to pull-down assays.

Again, RAD23B alone did not show any specific interaction with histone H3.1 (data not shown). To determine which part of XPC was involved in this interaction, we subjected the three truncated XPC proteins (one N-terminal and two C-terminal fragments, used in Fig. 4B,C) to pull-down assays. When a mixture of the three mutant XPC proteins was incubated with histone H3.1-bound beads, both C-terminal fragments, but not the N-terminal fragment, were specifically pulled down (Fig. 5B). Importantly, these interactions were also compromised by deletion of the N-terminal tail of histone H3.1.

The two C-terminal fragments of XPC contained the previously identified CETN2-binding site (amino acids 847–866) (Nishi *et al.* 2005). Therefore, we next addressed whether CETN2 binding affects this

Figure 4 Mapping of the histone-interacting domain in XPC. (A) Structural disorder probabilities were calculated and plotted for human XPC protein with two software packages, DISOPRED3 and DisProt (see also Bunick *et al.* 2006). Positions of known functional domains and truncated mutant proteins used in this study are shown. (B) Three FLAG-tagged XPC deletion mutants (N1, C1 and C2) were prepared and subjected to far-Western blot analysis with recombinant histone H3.1 [rH3.1 (+)]. As a control, the same set of samples was treated similarly, except that histone H3.1 was omitted from the incubation with the membrane filter [rH3.1 (−)]. (C) A similar experiment as (B), except that histone H1.2 was used instead of histone H3.1. (D and E) Far-Western blot analyses of a different set of His-tagged XPC deletion mutants (N1, N2 and N3) with histone H3.1 (D) or H1.2 (E).

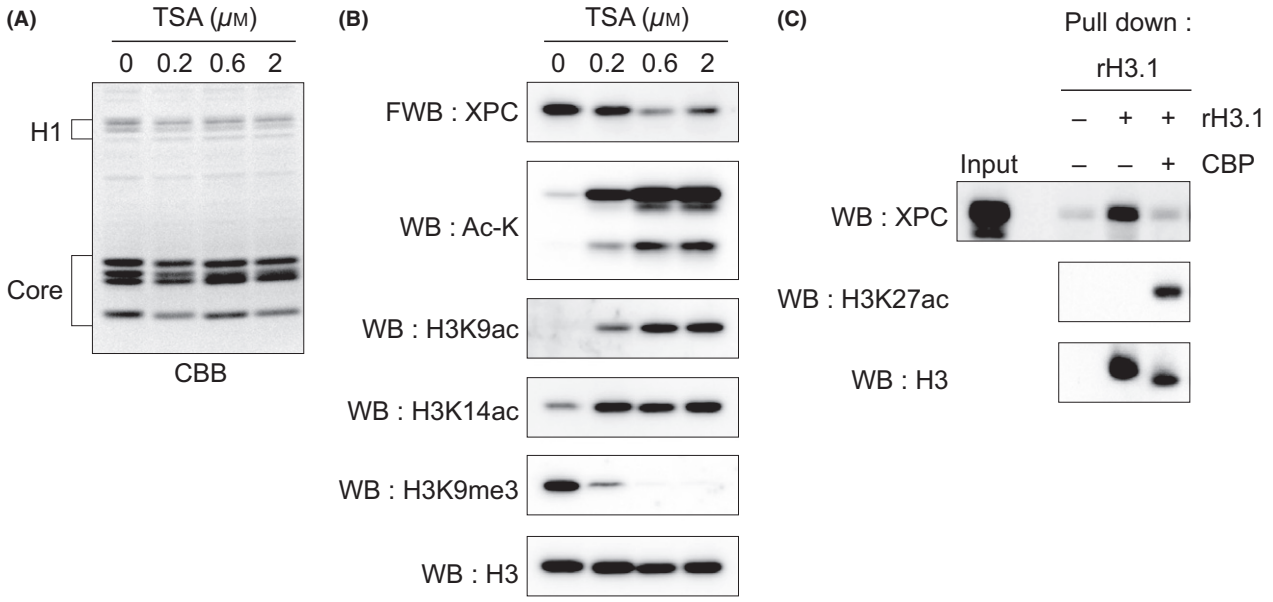

Figure 6 Acetylation of histone H3 attenuates interaction with XPC. (A) Cells were treated for 16 h with indicated concentrations of TSA. Total histone fractions were prepared and separated by SDS-PAGE followed by CBB staining. (B) Histone fractions shown in (A) were subjected to far-Western blot analysis with XPC–RAD23B and Western blot analyses with indicated antibodies. (C) *In vitro* acetylation was carried out with (+) or without (−) recombinant CBP and histone H3.1 immobilized on magnetic beads. After extensive washing, the beads were used to pull down XPC–RAD23B.

interaction between XPC and histone H3. For this purpose, purified recombinant CETN2 in molar excess was incubated with the XPC C-terminal fragment (513–870) in a crude insect cell extract. In this manner, a heterodimeric complex was efficiently reconstituted and purified, exactly as described for the XPC fragment alone (Fig. 5C). This complex formation did not affect the pull-down efficiency of the XPC C-terminal fragment, indicating that binding of CETN2 does not interfere with the interaction with histone H3 (Fig. 5D).

Acetylation of histone H3 attenuates interaction with XPC

As described above, HDAC activities are somehow involved in the process of damage recognition for GG-NER. Because our results indicated that the N-terminal tail of histone H3 was important for the interactions with XPC, we sought to determine whether the interactions are regulated by histone acetylation. To address this question, we first carried out far-Western blot analyses. Total histone fractions were prepared from cells treated with various concentrations of TSA (Fig. 6A). Western blot analyses confirmed that acetylated histones accumulated in a dose-dependent manner, whereas H3K9me3 was reduced reciprocally (Fig. 6B). When these histone fractions were subjected to far-Western blot analysis with XPC–RAD23B, the interaction of XPC with histone H3 was significantly weakened as the TSA concentration increased.

The effect of histone acetylation was further examined in a more defined system using recombinant proteins. Histone H3.1 immobilized on magnetic beads was treated with the recombinant histone acetyltransferase CBP and used to pull down the XPC–RAD23B complex. Induction of H3K27ac, a known product of acetylation by CBP (Tie *et al.* 2009), was confirmed, and CBP treatment substantially attenuated the interaction with XPC–RAD23B (Fig. 6C). Taken together, we conclude that the interaction between XPC and histone H3 is negatively regulated by acetylation of histone H3.

Taken together, the results described above raise the possibility that deacetylation of histone H3 is induced around sites containing DNA damage and could thus contribute to efficient recruitment of XPC. We tested this notion by subjecting cells to local UV irradiation through isopore membrane filters, followed by immunofluorescence staining of acetylated histone H3 (Fig. 7A). Accumulation of EGFP-XPC marked the areas with UV irradiation, and H3K27ac signals in the damaged areas tended to

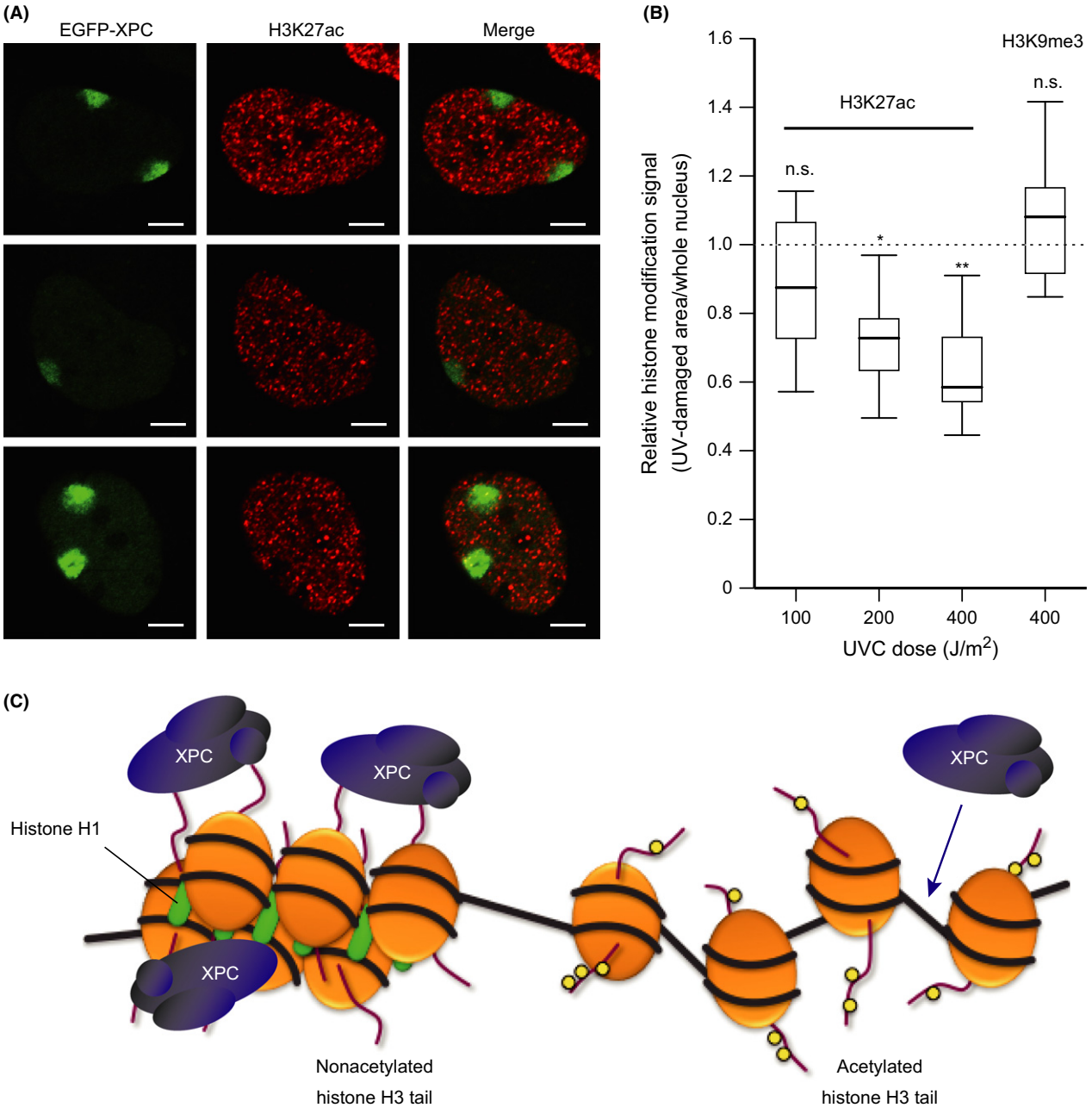

Figure 7 Local UVC irradiation induces reduction of H3K27ac. (A) XP4PASV cells stably expressing EGFP-XPC were irradiated with 400 J/m^2 UVC through isopore membrane filters (pore size, 5 μm). After 30-min incubation, the cells were fixed and immunostained with anti-H3K27ac antibody. Fluorescence images of EGFP (green) and Alexa Fluor 594 (red)-conjugated secondary antibody, together with merged images, are shown. Scale bar: 5 μm. (B) Local UVC irradiation at 100, 200 or 400 J/m^2 was applied to the cells expressing EGFP-XPC. After immunofluorescence staining with anti-H3K27ac antibody as in (A) (or anti-H3K9me3 antibody as a control), relative Alexa Fluor 594 fluorescence intensity per area was calculated for the site where EGFP-XPC was accumulated and divided by the value calculated for the whole nucleus. The ratios were calculated for at least 19 UV-irradiated areas from each sample, and the distributions are shown as box plots. Student's *t*-tests were carried out to assess whether the ratios were less than 1. *$P < 1 \times 10^{-6}$; **$P < 5 \times 10^{-9}$; n.s., not significant. (C) A model for regulation of the XPC localization in chromatin. XPC has at least two interfaces for interactions with the nonacetylated N-terminal tail of histone H3 and/or histone H1. In relatively open chromatin regions containing acetylated histone H3, the interaction of XPC would be more pronounced with non-nucleosomal DNA rather than with histones.

be lower than in the surrounding regions. Quantitative analyses confirmed that, in comparison with the whole nucleus, the local H3K27ac level in the UV-damaged area was significantly reduced in a dose-dependent manner, while similar reduction was not observed with other types of histone modifications, such as H3K9me3 (Fig. 7B). These results suggest that deacetylation of histone H3 occurs around the sites with UV-induced DNA damage.

Discussion

Possible roles of histone acetylation in GG-NER

Studies on roles of histone modifications in NER were pioneered by Smerdon *et al.* (1982), reporting that the treatment of cells with NaBu seemed to stimulate repair of UV-induced DNA damage. Subsequently, many published reports have pointed positive effects of histone acetylation on GG-NER (for review, see Li 2012). In contrast, our results showed in this study indicate that inhibition of HDAC activities compromised the process of DNA damage recognition by XPC and subsequent GG-NER (Fig. 2). One possible reason for such apparent inconsistency could be that we quantitatively assessed the repair kinetics of 6-4PPs and recruitment of damage recognition factors during relatively short periods after UV irradiation. In addition, our ChIP experiments indicated that XPC constitutively associates with chromatin, whereas UV-DDB inducibly and transiently binds to chromatin in response to UV irradiation of cells (Fig. 1; see also Matsumoto *et al.* 2015). Intriguingly, some types of acetylated histones, such as H3K14ac and H3K27ac, appear to be excluded from chromatin regions where XPC is bound, regardless of whether the cell has been exposed to UV irradiation. Therefore, the results of this study unexpectedly implicate deacetylated states of chromatin in regulating the localization and function of XPC.

Among histone acetylation at defined sites, H3K9ac has been implicated in recruitment of XPC and other NER factors to sites with UV-induced DNA damage, and the histone acetyltransferase GCN5 and the transcription factor E2F1 were shown to be involved in this process (Guo *et al.* 2010, 2011). Notably, however, it has not been directly explored at molecular levels how histone modifications affect dynamics of damage recognition factors and their interactions with DNA lesions. As found in regulation of transcription (Xhemalce & Kouzarides 2010), it would be conceivable that not all types of histone acetylation may have the same impact on GG-NER. According to our results, inhibition of HDACs did not completely block removal of 6-4PPs or accumulation of XPC to local UV damage. This is not surprising if a substantial fraction of UV photolesions is generated in chromatin regions that already lack relevant acetylated histones.

Although assembly of a lesion site into the nucleosome core inhibits recognition by XPC (Hara *et al.* 2000; Yasuda *et al.* 2005), we showed previously using a cell-free NER system that nucleosome formation in undamaged DNA masks nonspecific XPC–DNA interactions, thereby increasing the specificity of damage recognition (Yasuda *et al.* 2005). Analogously, hyperacetylated chromatin regions are probably more accessible to damage recognition factors but at the same time could allow nonspecific trapping of XPC by undamaged chromatin regions. Therefore, proper remodeling of chromatin structures around lesion sites in a spatiotemporally regulated manner may be crucial for efficient damage surveillance over the whole genome. This provides a possible explanation for our finding that global relaxation of chromatin by treatment with HDAC inhibitors was disadvantageous to GG-NER.

Given that deacetylation of histones is somehow induced at a lesion site, does it lead to condensation of neighboring chromatin structures? In fact, heterochromatin protein 1 accumulates upon local UV irradiation (Luijsterburg *et al.* 2009), suggesting that a heterochromatin-like structure is formed at least transiently. Apart from the preferential interaction of XPC with deacetylated histone H3, a possible role for such chromatin condensation around a lesion site is transient blockage of transcription and/or replication; it is conceivable that an encounter of the transcription or replication machinery with a site of ongoing NER must be deleterious to the cell. Although it remains unclear how NER could take place under such circumstances with condensed chromatin, it should be noted that heterochromatin has a highly dynamic nature (Wang *et al.* 2016).

Acetylated histone H3 was also underrepresented in DDB2-bound chromatin regions, but unlike XPC, accumulation of DDB2 to local UV damage was not significantly affected by treatment with HDAC inhibitors. One possible explanation for this is that, upon interacting with UV photolesions in chromatin, UV-DDB may immediately induce deacetylation of surrounding histones, which may then contribute to subsequent recruitment of XPC. However, accumulation of DDB2 upon local UV irradiation as well as

tethering of DDB2 at a defined genomic locus could induce chromatin decondensation (Luijsterburg *et al.* 2012; Adam *et al.* 2016), in which roles of histone acetylation remain to be established. Considering that DDB2 interacts with both HDAC (Zhao *et al.* 2014; Zhu *et al.* 2015) and histone acetyltransferases (Datta *et al.* 2001; Rapić-Otrin *et al.* 2002; Matsunuma *et al.* 2015), further studies are necessary to envisage UV-DDB-related regulation of histone acetylation and its role in GG-NER.

Physical interactions between XPC and histones

Recently, modes of damage search by XPC and its yeast homologue Rad4 have been examined *in vivo* and *in vitro* (Camenisch *et al.* 2009; Chen *et al.* 2015; Kong *et al.* 2016). The authors of these studies proposed that the BHD1/BHD2/β-turn interface of XPC engages in rapid interrogation of the DNA duplex via a sliding mechanism. A stable damage recognition complex is then formed by insertion of β-hairpin of BHD3 between the two DNA strands at the lesion site, and XPC must persist at a suspicious site for a sufficient time period to overcome a required energy barrier. Although this kinetic gating model for lesion recognition has been further supported and elaborated by more recent single-molecule imaging analyses (Kong *et al.* 2016), it remains to be determined how an efficient damage search is conducted by XPC in the context of chromatin structures. Previous photobleaching experiments showed that *in vivo* mobility of XPC is exceptionally low compared with other NER factors and sensitive to reduced temperature (Hoogstraten *et al.* 2008). This is inconsistent with a simple diffusion model; instead, it supports the notion that XPC probably searches for lesions through continuous association and dissociation on chromatin, which may require certain enzymatic activities such as ATP hydrolysis (Luijsterburg *et al.* 2012).

In this study, we found that XPC directly interacts with histones H3 and H1. Our far-Western blot analyses showed that the very N-terminal, unstructured region of XPC was important for interactions with both histones H3 and H1, whereas the C-terminal domains of XPC showed no detectable interactions. However, in pull-down assays with native forms of XPC, the C-terminal part of XPC was primarily responsible for interaction with histone H3, and no specific interactions involving the N-terminus of XPC and/or histone H1 were observed. Therefore, XPC appears to have at least two interfaces for binding to histones. We postulate that the major determinant of this interaction involves the C-terminal domains of XPC and histone H3 and depends on proper folding of XPC, whereas the interactions of the XPC N-terminus observed in far-Western blot analyses are relatively weak. Notably, binding of CETN2 did not interfere with the XPC–histone H3 interaction. Because CETN2 markedly augments the DNA-binding activities of XPC (Nishi *et al.* 2005), these results indicate that the heterotrimeric form of XPC is competent for interactions with both DNA and histones.

Importantly, deletion of the N-terminal tail of histone H3 severely compromised the interactions with both the N- and C-terminal regions of XPC, suggesting that the N-terminal tail of histone H3 serves as a platform for chromatin binding of XPC. Notably in this regard, in the crystal structure of the nucleosome core particle, the N-terminal tails of two histone H3 molecules protrude in the same direction around the entry and exit paths of DNA (Luger *et al.* 1997), where histone H1 (if present) is also thought to be deposited (Stützer *et al.* 2016). Thus, according to the beads-and-string model, putative XPC-interacting sites may be aligned along the axis of the nucleosome array. It is possible that such multifaceted interactions of XPC with histones could contribute to efficient damage search on chromatin fibers.

Another crucial aspect of the XPC–histone interactions is the effect of acetylation. In both far-Western blot analyses and pull-down assays, acetylation of histone H3 markedly weakened the interaction with XPC. This was consistent with our ChIP results, suggesting that XPC tends to be recruited preferentially to hypo-acetylated chromatin regions, where histone H1 is likely present as well (Stützer *et al.* 2016) (Fig. 7C). Notably, upon local UV irradiation through isopore membrane filters, the level of H3K27ac was reduced in the damaged areas, suggesting that deacetylation of histones may take place around lesion sites. Although such deacetylation may associate intrinsically with the GG-NER process (e.g., in a UV-DDB-dependent manner), blockage of replication and/or transcription at lesion sites could also induce local and transient chromatin condensation. Given that such chromatin condensation is accompanied by deacetylation of histones, it is possible that XPC is recruited to those sites, where it engages in initiation of NER. Further studies are required to elucidate the underlying molecular mechanisms and biological relevance of such deacetylation.

Experimental procedures

Cell culture

Simian virus 40-immortalized human fibroblast cell lines (normal cell line WI38 VA13 and *XPC*-deficient cell line XP4PASV) were cultured at 37 °C in a 5% CO_2 atmosphere in Dulbecco's modified Eagle medium (DMEM; Nissui Pharmaceutical, Tokyo, Japan) containing 10% fetal bovine serum (FBS). For selection of stably transformed cells, hygromycin B (Thermo Fisher Scientific, Waltham, MA, USA) or puromycin (Sigma-Aldrich, St Louis, MO, USA) was added at the indicated concentration. For baculovirus production, Sf9 cells were cultured at 27 °C with Grace's insect medium (supplemented; Thermo Fisher Scientific) containing 10% heat-inactivated FBS. Protein expression was carried out in High Five cells, which were maintained at 27 °C in Ex-Cell 405 serum-free medium (Sigma-Aldrich).

Chromatin immunoprecipitation

The XP4PASV transformant cell line stably expressing FLAG-tagged human XPC (FLAG-XPC) was established as described previously (Yasuda *et al.* 2007) and maintained in culture medium containing 10 μg/mL hygromycin B. A FLAG-tag was fused to the N-terminus of human DDB2 (FLAG-DDB2) and expressed in WI38 VA13 cells with the pIRESpuro2 vector (Takara Bio, Kusatsu, Shiga, Japan). Stably transformed cells were selected and maintained in the presence of 0.5 μg/mL puromycin.

For chromatin immunoprecipitation (ChIP), cells were seeded in 150-mm culture dishes (1–1.5 × 10^7 cells/dish), incubated overnight at 37 °C and irradiated with UVC at 10 J/m^2 (or sham-irradiated). After incubation for various periods of time, cells were fixed by adding 16% paraformaldehyde solution (methanol-free; Wako Pure Chemical, Osaka, Japan) to the culture medium at a final concentration of 1%, followed by incubation for 5 min at room temperature. The unreacted fixative was then quenched by adding glycine at a final concentration of 125 mM, followed by incubation for 5 min at room temperature. The fixed cells were washed with ice-cold phosphate-buffered saline (PBS) and scraped into buffer A [10 mM PIPES-NaOH (pH 6.8), 3 mM $MgCl_2$, 0.3 M NaCl, 1 mM EGTA, 0.1% Triton X-100, 33.3% sucrose, 10 mM *N*-ethylmaleimide (NEM), 10 mM sodium butyrate (NaBu)] containing protease inhibitor cocktail [0.25 mM phenylmethylsulfonyl fluoride (PMSF; Sigma-Aldrich), 1 μg/mL leupeptin (Roche Diagnostics, 2 μg/mL aprotinin (Roche Diagnostics), 1 μg/mL pepstatin (Roche Diagnostics, Basel, Switzerland), 50 μg/mL Pefabloc SC (AEBSF; Roche Diagnostics)]. The cell suspension was rotated at 4 °C for 1 h and centrifuged at 1000 ***g*** for 5 min. The resultant pellet was washed three times with buffer A, suspended in 200 μL of buffer B [10 mM Tris–HCl (pH 8.0), 0.14 M NaCl, 0.1% sodium dodecyl sulfate (SDS), 0.1% sodium deoxycholate, 1% Triton X-100, 10 mM NEM, 10 mM NaBu and protease inhibitor cocktail] and sonicated in a Bioruptor UCD-300 (Cosmo Bio, Tokyo, Japan) to obtain sheared DNA fragments 100–300 bp in length. After centrifugation at 20 000 ***g*** for 15 min, the supernatant fraction was subjected to immunoprecipitation with anti-FLAG M2 agarose beads (Sigma-Aldrich). The beads were washed extensively with buffer B, and the bound materials were eluted with buffer B containing 0.5 mg/mL FLAG peptide (Sigma-Aldrich).

Local UV irradiation

The XP4PASV transformant cell line stably expressing enhanced green fluorescent protein-tagged XPC (EGFP-XPC) was established as described previously (Nishi *et al.* 2009) and maintained in culture medium containing 10 μg/mL hygromycin B. Monomeric Kusabira Orange 1 was fused to the C-terminus of DDB2 (DDB2-mKO1), and the fusion protein was expressed in WI38 VA13 cells from the pMMPpuro retroviral expression vector (obtained from T. Taniguchi, Fred Hutchinson Cancer Research Center, with permission from R.C. Mulligan, Harvard Medical School). Stably transformed cells were selected and maintained in the presence of 0.5 μg/mL puromycin. Local UVC irradiation under a fluorescence microscope and quantitative measurement of fluorescence were carried out as described previously (Akita *et al.* 2015). UVC irradiation through a polycarbonate isopore membrane filter (5 μm pore size; Merck-Millipore, Darmstadt, Germany) was carried out as described (Yasuda *et al.* 2007).

Isolation of protein complexes containing XPC

The HA-FLAG tandem tag was fused to the N-terminus of XPC, and the fusion protein was stably expressed in HeLa S3 cells from the retroviral expression vector pOZ-N (Ikura *et al.* 2000). Nuclear extracts from cells expressing the fusion protein were subjected to sequential immunoprecipitation with anti-HA and anti-FLAG antibodies.

Preparation of chromatin and histone fractions from cultured cells

To prepare crude chromatin fractions, cells in a culture dish were washed with ice-cold PBS and scraped into buffer A containing protease inhibitor cocktail. The cell suspension was rotated at 4 °C for 1 h and centrifuged at 1000 ***g*** for 5 min. The resultant pellet was washed three times with buffer A containing protease inhibitor, and then sonicated in buffer B in a Bioruptor UCD-300. This suspension was used as the crude chromatin fraction.

The total histone fraction was prepared by the H_2SO_4 extraction method as described previously (Marunouchi *et al.* 1980) with several modifications. Instead of homogenization, cells in a culture dish were lysed *in situ* with buffer C [10 mM Tris–HCl (pH 7.5), 0.5 mM EDTA, 2 mM $MgCl_2$, 10 mM NaBu, 2 mM 3-mercapto-1, 2-propanediol (MPD; Wako Pure Chemical)] containing 0.1% Triton X-100. The lysate was collected with a cell scraper and centrifuged at 800 ***g*** for 5 min. The pellet was washed once with buffer C, resuspended in

buffer D [50 mM Tris–HCl (pH 7.5), 50 mM $NaHSO_3$, 1% MPD] and centrifuged at 9000 ***g*** for 5 min. The resultant pellet was resuspended in buffer D containing 0.15 M NaCl, incubated at 4 °C for 30 min and centrifuged at 9000 ***g*** for 5 min. Histone proteins were solubilized from the pellet with 0.2 M H_2SO_4 and recovered by precipitation with 20% trichloroacetic acid. To separate core and linker histones, the pellet obtained after the buffer D wash was resuspended in buffer D containing 0.6 M NaCl and incubated at 4 °C for 30 min. After centrifugation at 9000 ***g*** for 5 min, linker histones recovered in the supernatant were precipitated with 20% trichloroacetic acid, whereas core histones remaining in the pellet were solubilized and recovered as described above for total histones.

Purification of recombinant proteins

The heterodimeric complex of FLAG-XPC and RAD23B-His proteins was prepared as described previously (Nishi *et al.* 2005). The FLAG-tagged truncated XPC proteins were expressed in insect cells using the Bac-to-Bac baculovirus expression system (Thermo Fisher Scientific). High Five cells in a 150-mm culture dish were infected with a recombinant baculovirus and incubated at 27 °C for 2–3 days. The infected cells were collected, washed twice with PBS and suspended in eight packed cell volumes of buffer E [25 mM Tris–HCl (pH 8.0), 0.3 M NaCl, 1 mM EDTA, 10% glycerol, 1% Nonidet P-40 and protease inhibitor cocktail]. The cell lysate was incubated on ice for 30 min and centrifuged at 2300 ***g*** for 10 min. The resultant pellet was sonicated in buffer E and centrifuged at 9000 ***g*** for 10 min to obtain supernatant containing the truncated XPC protein. This extract was supplemented with Benzonase nuclease (at a final concentration of 5 U/mL; Merck-Millipore) and subjected to immunoprecipitation with anti-FLAG M2 agarose beads. After the beads were extensively washed with buffer F [20 mM sodium phosphate (pH 7.8), 1 M NaCl, 1 mM EDTA, 10% glycerol, 0.01% Triton X-100, 0.25 mM PMSF], bound proteins were eluted with the same buffer containing 0.5 mg/mL FLAG peptide. The CREB-binding protein fused to a C-terminal FLAG-tag (CBP-FLAG) was expressed in insect cells and purified with anti-FLAG M2 agarose beads (detailed purification procedures will be described elsewhere by T. Yasuda *et al.*).

The His-tagged XPC N-terminal fragments were expressed in *Escherichia coli* strain BL21 (DE3) with the pET-28a vector (Takara Bio). Inclusion bodies were solubilized by sonication in buffer G [50 mM Tris–HCl (pH 8.0), 0.3 M NaCl, 6 M urea, 5% glycerol], and the XPC fragments were purified with TALON metal affinity resin (Takara Bio). Recombinant histone H3.1 (full-length and N-terminal tail-less) (Tachiwana *et al.* 2011; Iwasaki *et al.* 2013), histone H1.2 (Machida *et al.* 2016) and CETN2 (Nishi *et al.* 2005) proteins were expressed in *E. coli* and purified as described previously.

Far-Western blot analysis

Proteins separated on a SDS polyacrylamide gel were transferred onto a polyvinylidene difluoride membrane filter (Immobilon-P; Merck-Millipore). The filter was first incubated with buffer H [10 mM Tris–HCl (pH 7.5), 0.1 M NaCl, 0.05% Tween 20] containing 5% skim milk (Wako Pure Chemical) to block nonspecific protein binding, and then with the recombinant protein of interest diluted in blocking solution. After overnight incubation at 4 °C, bound proteins were detected according to the standard methods for Western blot analysis using a secondary antibody conjugated to horseradish peroxidase (Medical & Biological Laboratories, Nagoya, Japan) and ImmunoStar LD (Wako Pure Chemical). Detection of chemiluminescence was carried out on a LAS-4010 lumino-imaging analyzer (GE Healthcare Biosciences, Piscataway, NJ, USA) and also with X-ray film (RX-U: Fujifilm, Tokyo, Japan).

Pull-down assay

To investigate interactions of nondenatured XPC proteins, 0.1 mg of paramagnetic beads conjugated to protein G (FG beads protein G; Tamagawa Seiki, Iida, Nagano, Japan) was incubated at 4 °C for 30 min with 1 μg of anti-histone H3 antibody (ab1791; Abcam) in 100 μL of PBS. After being washed with buffer I [20 mM Tris–HCl (pH 7.8), 2 M NaCl], the beads were further incubated at 4 °C for 1 h with 2 μg of recombinant histone H3.1 in 50 μL of buffer I. The beads were washed extensively with buffer I and used for subsequent binding reactions. For *in vitro* acetylation reactions, the beads bound to histone H3.1 were suspended in 50 μL of buffer J [50 mM Tris–HCl (pH 8.0), 1 mM EDTA, 10% glycerol, 1 mM DTT, 0.12 mM acetyl-CoA] and incubated at 30 °C for 2 h with 2.5 μg of CBP-FLAG.

Binding reactions were carried out at 4 °C for 1 h in 50 μL of buffer K [20 mM sodium phosphate (pH 7.8), 0.3 M NaCl, 10% glycerol, 0.1% Triton X-100, 0.2 mg/mL bovine serum albumin] containing 0.25 U/μL Benzonase nuclease. After the beads were washed extensively with buffer J, bound proteins were eluted by incubating at 37 °C for 30 min in SDS sample buffer [62.5 mM Tris–HCl (pH 6.8), 1% SDS, 1% MPD, 10% glycerol, 0.02% bromophenol blue].

Immunofluorescence staining

Cells in a 35-mm glass-bottom dish (poly-D-lysine-coated; MatTek, Ashland, MA, USA) were washed twice with PBS and fixed for 10 min at room temperature with 2% paraformaldehyde solution. The cells were washed twice with PBS and incubated for 10 min at room temperature in PBS containing 0.5% Triton X-100. After the cells were washed twice with PBS, PBS containing 2% FBS was added, and the sample was incubated for 30 min at room temperature to block nonspecific antibody binding. The cells were again washed twice with PBS and then incubated overnight at 4 °C with a primary antibody diluted in PBS containing 0.5% FBS. The cells were again washed twice with PBS and further incubated at 37 °C for 30 min with an appropriate secondary antibody labeled with Alexa Fluor (Thermo Fisher Scientific), diluted in PBS containing 0.5% FBS. After two more washes

in PBS, a coverslip was mounted with Vectashield mounting medium (Vector Laboratories, Burlingame, CA, USA). Immunofluorescence was observed on a LSM700 confocal laser scanning microscope (Carl Zeiss, Oberkochen, Germany). Quantitative analysis of the fluorescence intensities was carried out with the ImageJ software.

Other materials and methods

For transfection of cells with small interfering RNA (siRNA), the Lipofectamine RNAiMAX reagent (Thermo Fisher Scientific) was used, and the final concentration of siRNA in culture medium was adjusted at 20 nM. Quantitative measurement of UV-induced 6-4PPs in genomic DNA was carried out by enzyme-linked immunosorbent assay with lesion-specific monoclonal antibody (64M-2: Cosmo Bio), as described previously (Yasuda *et al*. 2007). To avoid dilution of lesions by DNA replication, cells were treated with 6 mM thymidine for 2 h before UV irradiation and also during the post-UV incubation.

Mouse monoclonal antibodies recognizing various histone modifications were purchased from MAB Institute (Sapporo, Hokkaido, Japan). For Western blotting, FLAG- and His-tagged proteins were detected using anti-DYDDDDK tag (1E5; Wako Pure Chemical) and anti-6 × Histidine (9C11; Wako Pure Chemical) monoclonal antibodies, respectively. Anti-XPC (Sugasawa *et al*. 2009) and anti-histone H1.2 (Machida *et al*. 2016) polyclonal antibodies were described in previous reports.

Acknowledgements

The authors are grateful to the members of Biosignal Research Center, and the Department of Biology, Graduate School of Science, Kobe University, for helpful discussions and encouragement. This work was supported by Grants-in-Aid to K.S. (JSPS KAKENHI Grant Numbers JP23116008, JP16H06307 and JP16H01311), to H. Kurumizaka (JSPS KAKENHI Grant Numbers JP25116002 and JP25250023), to T.I. (JSPS KAKENHI Grant Number JP16H01307) and to H. Kimura (JSPS KAKENHI Grant Number JP25116005). K.S. was also supported by a Grant for Environmental Research Projects from the Sumitomo Foundation (Grant Number 133084).

References

Adam, S., Dabin, J., Chevallier, O., Leroy, O., Baldeyron, C., Corpet, A., Lomonte, P., Renaud, O., Almouzni, G. & Polo, S.E. (2016) Real-time tracking of parental histones reveals their contribution to chromatin integrity following DNA damage. *Mol. Cell* **64**, 65–78.

Adam, S., Dabin, J. & Polo, S.E. (2015) Chromatin plasticity in response to DNA damage: the shape of things to come. *DNA Repair (Amst)* **32**, 120–126.

Akita, M., Tak, Y.S., Shimura, T., Matsumoto, S., Okuda-Shimizu, Y., Shimizu, Y., Nishi, R., Saitoh, H., Iwai, S., Mori, T., Ikura, T., Sakai, W., Hanaoka, F. & Sugasawa, K. (2015) SUMOylation of xeroderma pigmentosum group C protein regulates DNA damage recognition during nucleotide excision repair. *Sci. Rep.* **5**, 10984.

Araújo, S.J., Nigg, E.A. & Wood, R.D. (2001) Strong functional interactions of TFIIH with XPC and XPG in human DNA nucleotide excision repair, without a preassembled repairosome. *Mol. Cell. Biol.* **21**, 2281–2291.

de Boer, J. & Hoeijmakers, J.H.J. (2000) Nucleotide excision repair and human syndromes. *Carcinogenesis* **21**, 453–460.

Brown, K.L., Roginskaya, M., Zou, Y., Altamirano, A., Basu, A.K. & Stone, M.P. (2010) Binding of the human nucleotide excision repair proteins XPA and XPC/HR23B to the 5*R*-thymine glycol lesion and structure of the *cis*-(5*R*,6*S*) thymine glycol epimer in the 5′-GTgG-3′ sequence: destabilization of two base pairs at the lesion site. *Nucleic Acids Res.* **38**, 428–440.

Bunick, C.G., Miller, M.R., Fuller, B.E., Fanning, E. & Chazin, W.J. (2006) Biochemical and structural domain analysis of xeroderma pigmentosum complementation group C protein. *Biochemistry* **45**, 14965–14979.

Camenisch, U., Träutlein, D., Clement, F.C., Fei, J., Leitenstorfer, A., Ferrando-May, E. & Naegeli, H. (2009) Two-stage dynamic DNA quality check by xeroderma pigmentosum group C protein. *EMBO J.* **28**, 2387–2399.

Chen, X., Velmurugu, Y., Zheng, G., Park, B., Shim, Y., Kim, Y., Liu, L., Van Houten, B., He, C., Ansari, A. & Min, J.-H. (2015) Kinetic gating mechanism of DNA damage recognition by Rad4/XPC. *Nat. Commun.* **6**, 5849.

van Cuijk, L., van Belle, G.J., Turkyilmaz, Y., Poulsen, S.L., Janssens, R.C., Theil, A.F., Sabatella, M., Lans, H., Mailand, N., Houtsmuller, A.B., Vermeulen, W. & Marteijn, J.A. (2015) SUMO and ubiquitin-dependent XPC exchange drives nucleotide excision repair. *Nat. Commun.* **6**, 7499.

Datta, A., Bagchi, S., Nag, A., Shiyanov, P., Adami, G.R., Yoon, T. & Raychaudhuri, P. (2001) The p48 subunit of the damaged-DNA binding protein DDB associates with the CBP/p300 family of histone acetyltransferase. *Mutat. Res.* **486**, 89–97.

Fischer, E.S., Scrima, A., Böhm, K., Matsumoto, S., Lingaraju, G.M., Faty, M., Yasuda, T., Cavadini, S., Wakasugi, M., Hanaoka, F., Iwai, S., Gut, H., Sugasawa, K. & Thomä, N.H. (2011) The molecular basis of $CRL4^{DDB2/CSA}$ ubiquitin ligase architecture, targeting, and activation. *Cell* **147**, 1024–1039.

Fitch, M.E., Nakajima, S., Yasui, A. & Ford, J.M. (2003) *In vivo* recruitment of XPC to UV-induced cyclobutane pyrimidine dimers by the *DDB2* gene product. *J. Biol. Chem.* **278**, 46906–46910.

Friedberg, E.C. (2001) How nucleotide excision repair protects against cancer. *Nat. Rev. Cancer* **1**, 22–33.

Fujiwara, Y., Masutani, C., Mizukoshi, T., Kondo, J., Hanaoka, F. & Iwai, S. (1999) Characterization of DNA recognition by the human UV-damaged DNA-binding protein. *J. Biol. Chem.* **274**, 20027–20033.

Gillet, L.C.J. & Schärer, O.D. (2006) Molecular mechanisms of mammalian global genome nucleotide excision repair. *Chem. Rev.* **106**, 253–276.

Groisman, R., Polanowska, J., Kuraoka, I., Sawada, J., Saijo, M., Drapkin, R., Kisselev, A.F., Tanaka, K. & Nakatani, Y. (2003) The ubiquitin ligase activity in the DDB2 and CSA complexes is differentially regulated by the COP9 signalosome in response to DNA damage. *Cell* **113**, 357–367.

Guo, R., Chen, J., Mitchell, D.L. & Johnson, D.G. (2011) GCN5 and E2F1 stimulate nucleotide excision repair by promoting H3K9 acetylation at sites of damage. *Nucleic Acids Res.* **39**, 1390–1397.

Guo, R., Chen, J., Zhu, F., Biswas, A.K., Berton, T.R., Mitchell, D.L. & Johnson, D.G. (2010) E2F1 localizes to sites of UV-induced DNA damage to enhance nucleotide excision repair. *J. Biol. Chem.* **285**, 19308–19315.

Hanawalt, P.C. & Spivak, G. (2008) Transcription-coupled DNA repair: two decades of progress and surprises. *Nat. Rev. Mol. Cell Biol.* **9**, 958–970.

Hara, R., Mo, J. & Sancar, A. (2000) DNA damage in the nucleosome core is refractory to repair by human excision nuclease. *Mol. Cell. Biol.* **20**, 9173–9181.

Hey, T., Lipps, G., Sugasawa, K., Iwai, S., Hanaoka, F. & Krauss, G. (2002) The XPC-HR23B complex displays high affinity and specificity for damaged DNA in a true-equilibrium fluorescence assay. *Biochemistry* **41**, 6583–6587.

Hoogstraten, D., Bergink, S., Ng, J.M.Y., Verbiest, V.H.M., Luijsterburg, M.S., Geverts, B., Raams, A., Dinant, C., Hoeijmakers, J.H.J., Vermeulen, W. & Houtsmuller, A.B. (2008) Versatile DNA damage detection by the global genome nucleotide excision repair protein XPC. *J. Cell Sci.* **121**, 2850–2859.

Hwang, B.J., Ford, J.M., Hanawalt, P.C. & Chu, G. (1999) Expression of the *p48* xeroderma pigmentosum gene is p53-dependent and is involved in global genomic repair. *Proc. Natl Acad. Sci. USA* **96**, 424–428.

Ikura, T., Ogryzko, V.V., Grigoriev, M., Groisman, R., Wang, J., Horikoshi, M., Scully, R., Qin, J. & Nakatani, Y. (2000) Involvement of the TIP60 histone acetylase complex in DNA repair and apoptosis. *Cell* **102**, 463–473.

Iwasaki, W., Miya, Y., Horikoshi, N., Osakabe, A., Taguchi, H., Tachiwana, H., Shibata, T., Kagawa, W. & Kurumizaka, H. (2013) Contribution of histone N-terminal tails to the structure and stability of nucleosomes. *FEBS Open Bio* **3**, 363–369.

Jiang, Y., Wang, X., Bao, S., Guo, R., Johnson, D.G., Shen, X. & Li, L. (2010) INO80 chromatin remodeling complex promotes the removal of UV lesions by the nucleotide excision repair pathway. *Proc. Natl Acad. Sci. USA* **107**, 17274–17279.

Kapetanaki, M.G., Guerrero-Santoro, J., Bisi, D.C., Hsieh, C.L., Rapić-Otrin, V. & Levine, A.S. (2006) The DDB1-$CUL4A^{DDB2}$ ubiquitin ligase is deficient in xeroderma pigmentosum group E and targets histone H2A at UV-damaged DNA sites. *Proc. Natl Acad. Sci. USA* **103**, 2588–2593.

Kong, M., Liu, L., Chen, X., Driscoll, K.I., Mao, P., Böhm, S., Kad, N.M., Watkins, S.C., Bernstein, K.A., Wyrick, J.J., Min, J.-H. & Van Houten, B. (2016) Single-molecule imaging reveals that Rad4 employs a dynamic DNA damage recognition process. *Mol. Cell* **64**, 376–387.

Kulaksiz, G., Reardon, J.T. & Sancar, A. (2005) Xeroderma pigmentosum complementation group E protein (XPE/DDB2): purification of various complexes of XPE and analyses of their damaged DNA binding and putative DNA repair properties. *Mol. Cell. Biol.* **25**, 9784–9792.

Lagerwerf, S., Vrouwe, M.G., Overmeer, R.M., Fousteri, M.I. & Mullenders, L.H.F. (2011) DNA damage response and transcription. *DNA Repair (Amst)* **10**, 743–750.

Li, C.-L., Golebiowski, F.M., Onishi, Y., Samara, N.L., Sugasawa, K. & Yang, W. (2015) Tripartite DNA lesion recognition and verification by XPC, TFIIH, and XPA in nucleotide excision repair. *Mol. Cell* **59**, 1025–1034.

Li, R.-Y., Calsou, P., Jones, C.J. & Salles, B. (1998) Interactions of the transcription/DNA repair factor TFIIH and XP repair proteins with DNA lesions in a cell-free repair assay. *J. Mol. Biol.* **281**, 211–218.

Li, S. (2012) Implication of posttranslational histone modifications in nucleotide excision repair. *Int. J. Mol. Sci.* **13**, 12461–12486.

Luger, K., Mäder, A.W., Richmond, R.K., Sargent, D.F. & Richmond, T.J. (1997) Crystal structure of the nucleosome core particle at 2.8 A resolution. *Nature* **389**, 251–260.

Luijsterburg, M.S., Dinant, C., Lans, H. *et al.* (2009) Heterochromatin protein 1 is recruited to various types of DNA damage. *J. Cell Biol.* **185**, 577–586.

Luijsterburg, M.S., Lindh, M., Acs, K., Vrouwe, M.G., Pines, A., van Attikum, H., Mullenders, L.H. & Dantuma, N.P. (2012) DDB2 promotes chromatin decondensation at UV-induced DNA damage. *J. Cell Biol.* **197**, 267–281.

Machida, S., Hayashida, R., Takaku, M., Fukuto, A., Sun, J., Kinomura, A., Tashiro, S. & Kurumizaka, H. (2016) Relaxed chromatin formation and weak suppression of homologous pairing by the testis-specific linker histone H1T. *Biochemistry* **55**, 637–646.

Martinez, E., Palhan, V.B., Tjernberg, A., Lymar, E.S., Gamper, A.M., Kundu, T.K., Chait, B.T. & Roeder, R.G. (2001) Human STAGA complex is a chromatin-acetylating transcription coactivator that interacts with pre-mRNA splicing and DNA damage-binding factors in vivo. *Mol. Cell. Biol.* **21**, 6782–6795.

Marunouchi, T., Yasuda, H., Matsumoto, Y. & Yamada, M. (1980) Disappearance of a basic chromosomal protein from cells of a mouse temperature-sensitive mutant defective in histone phosphorylation. *Biochem. Biophys. Res. Commun.* **95**, 126–131.

Mathieu, N., Kaczmarek, N. & Naegeli, H. (2010) Strand- and site-specific DNA lesion demarcation by the xeroderma pigmentosum group D helicase. *Proc. Natl Acad. Sci. USA* **107**, 17545–17550.

Matsumoto, S., Fischer, E.S., Yasuda, T., Dohmae, N., Iwai, S., Mori, T., Nishi, R., Yoshino, K., Sakai, W., Hanaoka,

F., Thomä, N.H. & Sugasawa, K. (2015) Functional regulation of the DNA damage-recognition factor DDB2 by ubiquitination and interaction with xeroderma pigmentosum group C protein. *Nucleic Acids Res.* **43**, 1700–1713.

Matsunuma, R., Niida, H., Ohhata, T., Kitagawa, K., Sakai, S., Uchida, C., Shiotani, B., Matsumoto, M., Nakayama, K.I., Ogura, H., Shiiya, N. & Kitagawa, M. (2015) UV damage-induced phosphorylation of HBO1 triggers $CRL4^{DDB2}$-mediated degradation to regulate cell proliferation. *Mol. Cell. Biol.* **36**, 394–406.

Min, J.-H. & Pavletich, N.P. (2007) Recognition of DNA damage by the Rad4 nucleotide excision repair protein. *Nature* **449**, 570–575.

Moser, J., Volker, M., Kool, H., Alekseev, S., Vrieling, H., Yasui, A., van Zeeland, A.A. & Mullenders, L.H.F. (2005) The UV-damaged DNA binding protein mediates efficient targeting of the nucleotide excision repair complex to UV-induced photo lesions. *DNA Repair (Amst)* **4**, 571–582.

Nishi, R., Alekseev, S., Dinant, C., Hoogstraten, D., Houtsmuller, A.B., Hoeijmakers, J.H.J., Vermeulen, W., Hanaoka, F. & Sugasawa, K. (2009) UV-DDB-dependent regulation of nucleotide excision repair kinetics in living cells. *DNA Repair (Amst)* **8**, 767–776.

Nishi, R., Okuda, Y., Watanabe, E., Mori, T., Iwai, S., Masutani, C., Sugasawa, K. & Hanaoka, F. (2005) Centrin 2 stimulates nucleotide excision repair by interacting with xeroderma pigmentosum group C protein. *Mol. Cell. Biol.* **25**, 5664–5674.

Nishi, R., Sakai, W., Tone, D., Hanaoka, F. & Sugasawa, K. (2013) Structure-function analysis of the EF-hand protein centrin-2 for its intracellular localization and nucleotide excision repair. *Nucleic Acids Res.* **41**, 6917–6929.

Okuda, M., Kinoshita, M., Kakumu, E., Sugasawa, K. & Nishimura, Y. (2015) Structural insight into the mechanism of TFIIH recognition by the acidic string of the nucleotide excision repair factor XPC. *Structure* **23**, 1827–1837.

Osakabe, A., Tachiwana, H., Kagawa, W., Horikoshi, N., Matsumoto, S., Hasegawa, M., Matsumoto, N., Toga, T., Yamamoto, J., Hanaoka, F., Thomä, N.H., Sugasawa, K., Iwai, S. & Kurumizaka, H. (2015) Structural basis of pyrimidine-pyrimidone (6-4) photoproduct recognition by UV-DDB in the nucleosome. *Sci. Rep.* **5**, 16330.

Payne, A. & Chu, G. (1994) Xeroderma pigmentosum group E binding factor recognizes a broad spectrum of DNA damage. *Mutat. Res.* **310**, 89–102.

Pines, A., Vrouwe, M.G., Marteijn, J.A., Typas, D., Luijsterburg, M.S., Cansoy, M., Hensbergen, P., Deelder, A., de Groot, A., Matsumoto, S., Sugasawa, K., Thoma, N., Vermeulen, W., Vrieling, H. & Mullenders, L. (2012) PARP1 promotes nucleotide excision repair through DDB2 stabilization and recruitment of ALC1. *J. Cell Biol.* **199**, 235–249.

Polo, S.E. & Almouzni, G. (2015) Chromatin dynamics after DNA damage: the legacy of the access-repair-restore model. *DNA Repair (Amst)* **36**, 114–121.

Poulsen, S.L., Hansen, R.K., Wagner, S.A., van Cuijk, L., van Belle, G.J., Streicher, W., Wikström, M., Choudhary, C., Houtsmuller, A.B., Marteijn, J.A., Bekker-Jensen, S. & Mailand, N. (2013) RNF111/Arkadia is a SUMO-targeted ubiquitin ligase that facilitates the DNA damage response. *J. Cell Biol.* **201**, 797–807.

Puumalainen, M.-R., Lessel, D., Rüthemann, P., Kaczmarek, N., Bachmann, K., Ramadan, K. & Naegeli, H. (2014) Chromatin retention of DNA damage sensors DDB2 and XPC through loss of p97 segregase causes genotoxicity. *Nat. Commun.* **5**, 3695.

Rapić-Otrin, V., McLenigan, M.P., Bisi, D.C., Gonzalez, M. & Levine, A.S. (2002) Sequential binding of UV DNA damage binding factor and degradation of the p48 subunit as early events after UV irradiation. *Nucleic Acids Res.* **30**, 2588–2598.

Reardon, J.T., Nichols, A.F., Keeney, S., Smith, C.A., Taylor, J.-S., Linn, S. & Sancar, A. (1993) Comparative analysis of binding of human damaged DNA-binding protein (XPE) and *Escherichia coli* damage recognition protein (UvrA) to the major ultraviolet photoproducts: T[c, s]T, T[t, s]T, T[6-4]T, and T[Dewar]T. *J. Biol. Chem.* **268**, 21301–21308.

Robu, M., Shah, R.G., Petitclerc, N., Brind'Amour, J., Kandan-Kulangara, F. & Shah, G.M. (2013) Role of poly(ADP-ribose) polymerase-1 in the removal of UV-induced DNA lesions by nucleotide excision repair. *Proc. Natl Acad. Sci. USA* **110**, 1658–1663.

Schärer, O.D. (2013) Nucleotide excision repair in eukaryotes. *Cold Spring Harb. Perspect. Biol.* **5**, a012609.

Scrima, A., Konícková, R., Czyzewski, B.K., Kawasaki, Y., Jeffrey, P.D., Groisman, R., Nakatani, Y., Iwai, S., Pavletich, N.P. & Thomä, N.H. (2008) Structural basis of UV DNA-damage recognition by the DDB1-DDB2 complex. *Cell* **135**, 1213–1223.

Shiyanov, P., Nag, A. & Raychaudhuri, P. (1999) Cullin 4A associates with the UV-damaged DNA-binding protein DDB. *J. Biol. Chem.* **274**, 35309–35312.

Smerdon, M.J., Lan, S.Y., Calza, R.E. & Reeves, R. (1982) Sodium butyrate stimulates DNA repair in UV-irradiated normal and xeroderma pigmentosum human fibroblasts. *J. Biol. Chem.* **257**, 13441–13447.

Stützer, A., Liokatis, S., Kiesel, A., Schwarzer, D., Sprangers, R., Söding, J., Selenko, P. & Fischle, W. (2016) Modulations of DNA contacts by linker histones and post-translational modifications determine the mobility and modifiability of nucleosomal H3 tails. *Mol. Cell* **61**, 247–259.

Sugasawa, K., Akagi, J., Nishi, R., Iwai, S. & Hanaoka, F. (2009) Two-step recognition of DNA damage for mammalian nucleotide excision repair: directional binding of the XPC complex and DNA strand scanning. *Mol. Cell* **36**, 642–653.

Sugasawa, K., Okamoto, T., Shimizu, Y., Masutani, C., Iwai, S. & Hanaoka, F. (2001) A multistep damage recognition mechanism for global genomic nucleotide excision repair. *Genes Dev.* **15**, 507–521.

Sugasawa, K., Okuda, Y., Saijo, M., Nishi, R., Matsuda, N., Chu, G., Mori, T., Iwai, S., Tanaka, K., Tanaka, K. &

Hanaoka, F. (2005) UV-induced ubiquitylation of XPC protein mediated by UV-DDB-ubiquitin ligase complex. *Cell* **121**, 387–400.

Sugasawa, K., Shimizu, Y., Iwai, S. & Hanaoka, F. (2002) A molecular mechanism for DNA damage recognition by the xeroderma pigmentosum group C protein complex. *DNA Repair (Amst)* **1**, 95–107.

Tachiwana, H., Kagawa, W., Shiga, T., Osakabe, A., Miya, Y., Saito, K., Hayashi-Takanaka, Y., Oda, T., Sato, M., Park, S.-Y., Kimura, H. & Kurumizaka, H. (2011) Crystal structure of the human centromeric nucleosome containing CENP-A. *Nature* **476**, 232–235.

Tang, J.Y., Hwang, B.J., Ford, J.M., Hanawalt, P.C. & Chu, G. (2000) Xeroderma pigmentosum *p48* gene enhances global genomic repair and suppresses UV-induced mutagenesis. *Mol. Cell* **5**, 737–744.

Tie, F., Banerjee, R., Stratton, C.A., Prasad-Sinha, J., Stepanik, V., Zlobin, A., Diaz, M.O., Scacheri, P.C. & Harte, P.J. (2009) CBP-mediated acetylation of histone H3 lysine 27 antagonizes *Drosophila* Polycomb silencing. *Development* **136**, 3131–3141.

Wang, H., Zhai, L., Xu, J., Joo, H.Y., Jackson, S., Erdjument-Bromage, H., Tempst, P., Xiong, Y. & Zhang, Y. (2006) Histone H3 and H4 ubiquitylation by the CUL4-DDB-ROC1 ubiquitin ligase facilitates cellular response to DNA damage. *Mol. Cell* **22**, 383–394.

Wang, J., Jia, S.T. & Jia, S. (2016) New insights into the regulation of heterochromatin. *Trends Genet.* **32**, 284–294.

Wang, Q.E., Zhu, Q., Wani, G., Chen, J. & Wani, A.A. (2004) UV radiation-induced XPC translocation within chromatin is mediated by damaged-DNA binding protein, DDB2. *Carcinogenesis* **25**, 1033–1043.

Wittschieben, B.Ø., Iwai, S. & Wood, R.D. (2005) DDB1-DDB2 (xeroderma pigmentosum group E) protein complex recognizes a cyclobutane pyrimidine dimer, mismatches, apurinic/apyrimidinic sites, and compound lesions in DNA. *J. Biol. Chem.* **280**, 39982–39989.

Xhemalce, B. & Kouzarides, T. (2010) A chromodomain switch mediated by histone H3 Lys 4 acetylation regulates heterochromatin assembly. *Genes Dev.* **24**, 647–652.

Yang, W. (2008) Structure and mechanism for DNA lesion recognition. *Cell Res.* **18**, 184–197.

Yasuda, G., Nishi, R., Watanabe, E., Mori, T., Iwai, S., Orioli, D., Stefanini, M., Hanaoka, F. & Sugasawa, K. (2007) In vivo destabilization and functional defects of the xeroderma pigmentosum C protein caused by a pathogenic missense mutation. *Mol. Cell. Biol.* **27**, 6606–6614.

Yasuda, T., Sugasawa, K., Shimizu, Y., Iwai, S., Shiomi, T. & Hanaoka, F. (2005) Nucleosomal structure of undamaged DNA regions suppresses the non-specific DNA binding of the XPC complex. *DNA Repair (Amst)* **4**, 389–395.

Yeo, J.E., Khoo, A., Fagbemi, A.F. & Schärer, O.D. (2012) The efficiencies of damage recognition and excision correlate with duplex destabilization induced by acetylaminofluorene adducts in human nucleotide excision repair. *Chem. Res. Toxicol.* **25**, 2462–2468.

Yokoi, M., Masutani, C., Maekawa, T., Sugasawa, K., Ohkuma, Y. & Hanaoka, F. (2000) The xeroderma pigmentosum group C protein complex XPC-HR23B plays an important role in the recruitment of transcription factor IIH to damaged DNA. *J. Biol. Chem.* **275**, 9870–9875.

Zhao, R., Han, C., Eisenhauer, E., Kroger, J., Zhao, W., Yu, J., Selvendiran, K., Liu, X., Wani, A.A. & Wang, Q.-E. (2014) DNA damage-binding complex recruits HDAC1 to repress Bcl-2 transcription in human ovarian cancer cells. *Mol. Cancer Res.* **12**, 370–380.

Zhu, Q., Battu, A., Ray, A., Wani, G., Qian, J., He, J., Wang, Q.-E. & Wani, A.A. (2015) Damaged DNA-binding protein down-regulates epigenetic mark H3K56Ac through histone deacetylase 1 and 2. *Mutat. Res.* **776**, 16–23.

Received: 4 January 2017
Accepted: 13 January 2017